

Relationship between ERS Scatterometer Measurement and Integrated Wind and Wave Parameters

Y. QUILFEN AND B. CHAPRON

Département d'Océanographie Spatiale, Centre de Brest, IFREMER, Plouzané, France

F. COLLARD

BOOST-Technologies, Plouzané, France

D. VANDEMARK

NASA Goddard Space Flight Center, Wallops Flight Facility, Laboratory for Hydrospheric Processes, Wallops Island, Virginia

18 April 2003 and 30 August 2003

ABSTRACT

Potential effects of environmental parameters such as sea state or atmospheric boundary layer stability on the normalized radar cross section (NRCS) measured by spaceborne sensors have been investigated for a long time. Using neural networks and large high quality collocated datasets, the relation between the European Remote Sensing Satellite (ERS) C-band scatterometer NRCS measurement and integrated sea state parameters (i.e., the mean wave period and significant wave height) measured by buoys is studied. As anticipated, NRCS measurements correlate well with an empirically derived parameter H^a/T^b , revealing the mean bulk relationship between a mean 10-m wind speed and the corresponding sea state development. The correlation and exponents exhibit dependency on the scatterometer incidence angles. A neural model that relates the scatterometer NRCS measurements to these wave spectral integrated parameters and wind speed is also developed. As obtained, the retrieval skill is significantly improved, by comparison with operational empirical models such as CMOD-IFR2 or CMOD4, when including wave effects. As illustrated, systematic biases occur under particular environmental conditions when using the operational scatterometer backscatter model functions.

1. Introduction

Model functions relating measured altimeter and scatterometer normalized radar cross sections (NRCSs) to near-surface wind have been thoroughly tested over the past years. Requirements are met, but studies based on collocated satellite, model, and/or in situ estimates still reveal relatively large scatter (Graber et al. 1996). Measurements and numerical predictions, as well as the empirical model functions, do contain errors. For altimeter and scatterometer instruments, cases of erroneous wind inversions have been documented and shown to be related to the presence of surface currents, surfactant, temperature fronts, atmospheric stratification, and precipitation (e.g., Keller et al. 1989; Vandemark et al. 1997; Weissman and Graber 1999). There is also evidence that the sea state maturity can affect the radar measurements. Indeed, experimental results show that the ocean's drag

coefficient depends on sea state (e.g., Donelan et al. 1993) to influence the wind stress and to impact small-scale roughness development, and thus the measured backscatter intensity. An increasing influence of the surface drift on short-wave dissipation (e.g., Banner and Phillips 1974; Quilfen et al. 1999) can also be invoked to suggest that local sea state conditions (current, sea state maturity, wind/swell direction alignment) will impact radar wind inversion. This sea state influence on altimeter measurements is already well documented (Chen et al. 2000; Queffeulou et al. 1999; Gourrion et al. 2002a,b). Theoretical backscattering models accounting for sea state effects, crucial to physical understanding, have also been developed but show limited skills for operational purposes. To our knowledge, an empirical development taking into account a sea state parameter has only been successfully derived for Ku-band altimeters and is currently operational for the altimeter wind inversion (Gourrion et al. 2002a,b).

In this note, we focus on C-band scatterometer data. A neural model is developed to relate the radar cross section to both surface wind and sea state information. As tested, this provides significant improvement on scat-

Corresponding author address: Dr. Yves Quilfen, Département d'Océanographie Spatiale, Centre de Brest, IFREMER, Technopole de Brest-Iroise, B. P. 70, 29280 Plouzané, France.
E-mail: yves.quilfen@ifremer.fr

terometer-retrieved wind estimates. In section 2, the datasets and methods used in the study are presented. In section 3, an analysis of the relationship between European Remote Sensing Satellite (ERS) C-band measurements and the integrated wind and sea state parameters is given. In section 4, illustrations are shown to reveal strong local effects and obtained improvements. Discussion follows in section 5.

2. Data and methods

The analyses are based upon sets of *ERS-1* and -2 scatterometer measurements collocated with the National Data Buoy Center (NDBC) buoys. Scatterometer data are processed offline at the French Research Institute for Exploitation of the Sea (IFREMER) using the CMOD-IFR2 backscattering model to compute the 10-m neutral wind (Quilfen et al. 1998). The NDBC data have been collected over the period September 1992–January 2001 by 48 buoys. These buoy measurements are converted to 10-m neutral winds using a log-profile relation accounting for the atmospheric stability. In this study, the closest buoy 1-h average estimates to the time of *ERS-1* or -2 overpass is collocated with scatterometer data. The separation distance between measurements is less than 25 km. As found, 36 218 collocated data pairs have been compiled. We take the convention that “wind speed” stands for the neutral stability wind measured at 10-m height.

Taking advantage of buoy wave measurements, we use a methodology based upon neural networks to define the geophysical model function (GMF) relating the scatterometer NRCSs to the buoy wind and wave parameters. The procedures used are those of the MATLAB neural toolbox (The MathWorks, Inc.).

3. Relation of NRCS with the integrated wind and wave parameters

We first establish the link between the NRCSs and the sea state parameters. This helps to derive a neural model and interpret the relationship between the NRCSs and both the wind and wave parameters.

a. The NRCS to integrated wave parameters relation

We develop and train the following neural model:

$$\sigma_1 + \sigma_3 = a \left(\frac{H^\alpha}{T^\beta} \right) + b, \quad (1)$$

where H and T are the buoy-integrated significant wave height and mean wave period, respectively; α and β are constant exponents; σ_1 and σ_3 stand for the aft and fore beam NRCSs, respectively; and a and b are incidence angle dependent coefficients. The sum of the aft and fore beam NRCSs filters out most of the wind direction effects.

As understood, a wind blowing over the ocean surface will rapidly roughen the surface. With time or fetch, the sea develops and similarity laws apply (e.g., Kitaigorodskii 1973). Thus, on average, backscatter measurements are expected to correlate with integrated sea state parameters. The choice of the parameter H^α/T^β also comes from previous results, showing that C-band model residuals (observed minus predicted NRCS) are correlated with such a parameter (Quilfen et al. 2001).

The neural model outputs are the two exponents α and β , and the simulated NRCS. Evaluations are performed from data subsets at the different incidence angles corresponding to the 19 scatterometer nodes covering the swath across the satellite track. In Fig. 1a, we observe nearly constant values for the exponents, except at the lowest incidence angles, where values are slightly lower. Mean values are close to 1.5 and 2.5 for α and β , respectively. As obtained, the NRCS dependency is not strictly related to a significant slope parameter ($\sim H/T^2$). According to the exponent values, it is rather a combination (product) of the significant slope and the square root of the significant velocity ($\sim H/T$) parameter. Finally, since the CMOD-IFR2 model roughly predicts the NRCS to depend on the square root of the wind speed, these exponent values are very consistent with the known high correlation of nondimensional wind sea energy to inverse wave age (Hanson and Phillips 1999; Donelan et al. 1992). Specifically, these studies have led to the relationship

$$\frac{H^2}{T^\gamma} \sim U^{4-\gamma}, \quad (2)$$

where γ is a constant. With $(\sigma_1 + \sigma_3) \sim U^{0.5}$ and the two exponents values found in this study, we find $\gamma \sim 3.3$. This γ value matches exactly the Lake St. Clair (Michigan/Ontario, Canada) observations of Donelan et al. (1992). It also confirms the approximate NRCS square root wind dependency. Recovering such a relationship using scatterometer data thus confirms the relatively marginal impact of swell-dominated open ocean conditions on scatterometer measurements for moderate to high wind conditions. These results imply that, statistically, sea state contributions not directly associated with the local forcing are certainly of second order. However, it must be noticed that at the lowest incidence angles, the α and β exponent values are different and tend to $\beta \approx 2\alpha$. As mentioned above, this corresponds to proportionality with an integrated significant slope parameter. Accordingly, for these incidences, deviations from mean swell steepness conditions shall certainly more significantly impact C-band scatterometer signals. The incidence-angle dependency is further illustrated in Fig. 1b. Residuals of the neural process (least squares errors) and the correlation coefficient between the neural model and the measurements are presented. Recall that the integrated wave parameters H and T are computed from the 0.03–0.4 Hz frequency range and are therefore

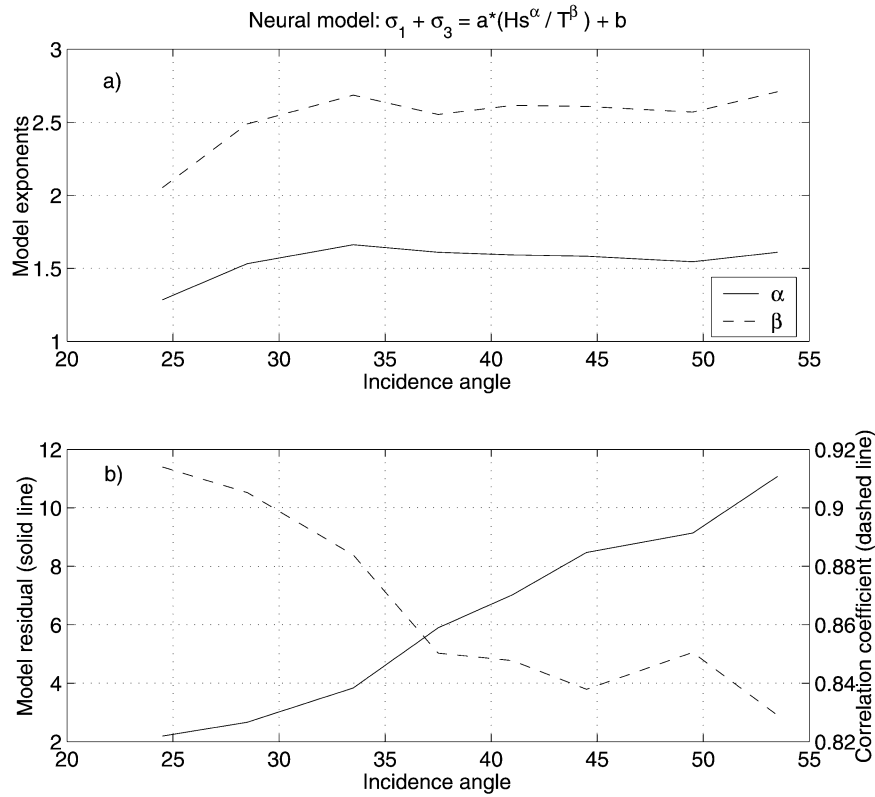


FIG. 1. (a) Neural model exponents, α (solid line) and β (dashed line), as a function of incidence. (b) Associated model residuals (solid line, the residual of the least square minimization process fitting modeled and measured NRCS) and correlation coefficient (dashed line) between modeled and measured NRCS.

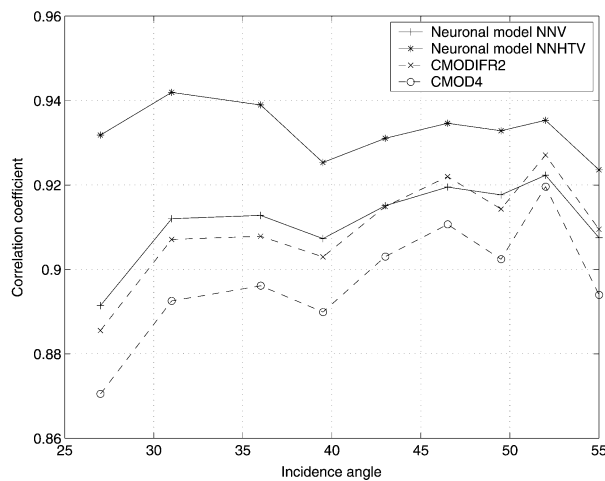


FIG. 2. Correlation coefficient between modeled and measured NRCS as a function of incidence angle: NNV (solid line stars), NNHTV (solid line plus signs), CMOD-IFR2 (dashed line/crosses), CMOD4 (dashed line/circles).

related to gravity waves longer than 10 m. While correlation is still remarkably high, it is apparent that scatterometer measurements at higher incidence angles are less correlated to these integrated larger-scale spectral moments.

b. Evaluation of different neural models

We further define and train neural models with the wind and wave parameters as inputs. In addition to the one discussed in section 3a, two models have been defined. The first, denoted as NNV, solely accounts for the NRCS dependency on the 10-m wind speed. The second, denoted as NNHTV, accounts for the wind speed, the wave height, and average period. As shown in Fig. 2, the NNV model compares favorably with the operational models, CMOD-IFR2 and CMOD4, giving a slightly better correlation with the measured NRCS. It demonstrates the robustness of the neural approach in our analysis. The NNV model does show a slight trend as a function of the incidence angle. Correlations slightly increase with the incidence angle. It again reflects the fact that large-scale induced tilting effects add a more significant contribution at low incidence angles, which decreases the relative contribution of the pure

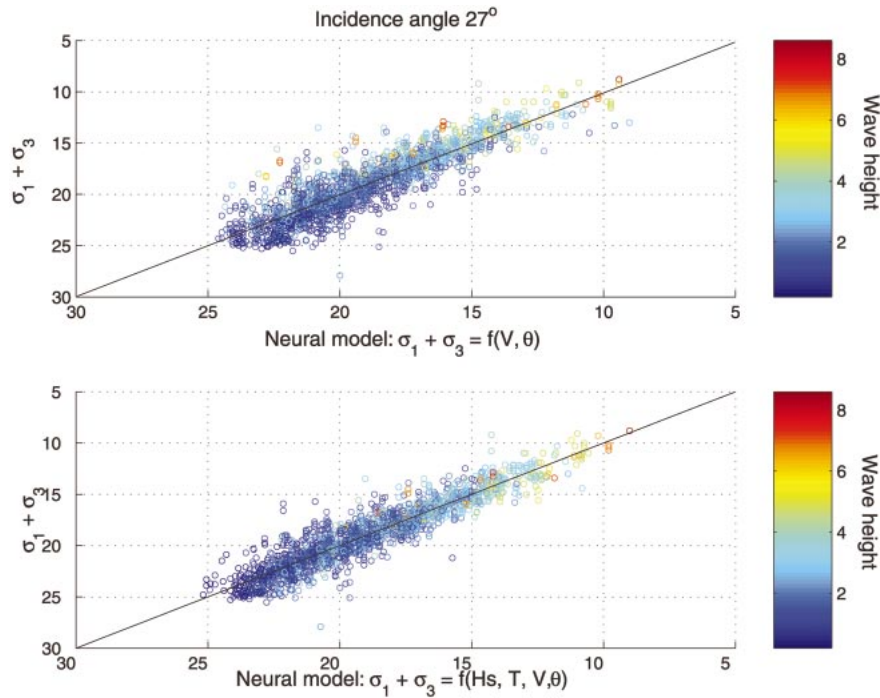


FIG. 3. Scatterplots comparing the measured (y axis) and modeled (x axis) NRCS using (top) NNV and (bottom) NNHTV for an incidence angle of 27° . Each circle represents one measurement, color coded as a function of the significant wave height.

wind-induced surface waves to the return signal. Adding the spectral parameters with NNHTV improves the results for all incidence angles, with a marked effect at lower incidence angles. The correlation coefficient is now almost incidence-angle independent and above 0.92 everywhere. Such high correlation levels come from a combination of different factors: very effective analysis tools, that is, very precise buoy/scatterometer collocation and neural network adequacy, and very low radiometric resolution at C band. It clearly reflects the scatterometer potential to integrate the wind and wave conditions in the NRCS measurements, to provide information on the wave field in addition to that on the wind field. The results illustrated by the NNHTV model also indicate that wind speed retrieval can be improved. A neural network, NNVH not taking into account the period parameter, was also tested (not shown). Correlations also increase by comparison with NNV but are lower than those obtained with NNHTV. This is in agreement with the previous study by Quilfen et al. (2001), which NRCS errors were found to be significantly better correlated with wave parameters when the period was accounted for. Indeed, the significant wave height is only a relatively poor descriptor of the wind wave field that affects the scatterometer measurements. However, for operational purposes, and because measurements of the significant wave height are readily available from altimeters, it may be anticipated that wind estimates can be also improved when including

the significant wave height alone, in addition to the wind vector, in the backscatter model.

4. Evidence of local sea state effects on the C-band scatterometer NRCSs

The analysis performed in the previous section is a global one, averaging over the whole wind speed range and fetch conditions. The potential impact of waves on the scatterometer measurements are certainly much larger in specific conditions such as falling or rising wind conditions, and anomalous sea state degree of development.

Figures 3 and 4 present scatterplots of the measured NRCS and the NRCS modeled with NNV (top) and NNHTV (bottom) for two incidence angles, 27° and 37° , respectively. The measurements are color-coded as a function of the significant wave height. When considering the NNV plots, a few outliers are found at both low and high winds. At lower wind speeds, there are cases where NRCS measurements (the sum of the aft and fore beams) differ by as much as 5 dB from the NNV model. These observations are associated with high significant wave heights. NRCS underestimation by the NNV model results in a large overestimation of the retrieved wind speed. Oppositely, at high winds, measurements corresponding to low values of the significant wave height lie under the model predictions. In such cases, under-estimation of the retrieved wind speed

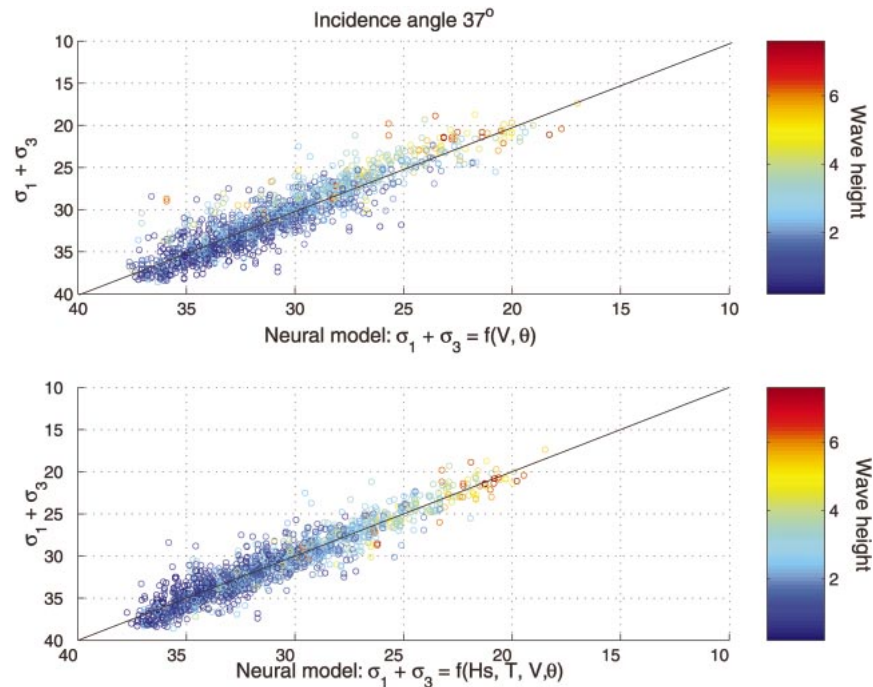


FIG. 4. Scatterplots comparing the measured (y axis) and modeled (x axis) NRCS using (top) NNV and (bottom) NNHTV for an incidence angle of 37° . Each circle represents one measurement, color coded as a function of the significant wave height.

follows. These situations are associated with particular conditions, that is, residual sea state and non-fully developed seas, respectively. Taking into account the wave spectral parameters in NNHTV lowers these impacts to correctly model the NRCS. The same features are observed in Fig. 4 at incidence angle 37° . This figure also reveals anomalies that occur over the whole wind speed range. The improvements obtained with the NNHTV model apply for the whole wind speed range.

5. Summary

Sea state conditions certainly affect measurements made by scatterometers. The importance of including sea state parameters in model inversion is still open for debate, but increased correlations have been obtained when considering large-scale integrated wave parameters. Compared to previous attempts, this study certainly benefits from the large number of high quality collocated datasets. While the impact of various sea state parameters (wave age, wave height, etc.) has been thoroughly studied from field experiments, such a unique dataset enables us to derive practical empirical models to be tested further. These first results are encouraging and of interest both in the pursuit of a better understanding of how short and long waves interact and for the practical purpose of developing algorithms to infer wind and wind stress from scatterometer measurements and also from synthetic aperture radar data. In particular, for the lowest incidence angles, the sea state steepness

shall be accounted for. As foreseen, information provided by a wave forecast and/or altimeter measurements may be included in such empirical wind retrieval algorithms. As suggested, a simple extension shall be to include information on one or possibly two integrated parameters. Following this development, small but systematic well-defined seasonal and regional biases should be better detected to assess accuracy of ocean surface wind and wind stress forcing fields.

REFERENCES

- Banner, M. L., and O. M. Phillips, 1974: On the incipient breaking of small scale waves. *J. Fluid Mech.*, **4**, 647–656.
- Chen, G., H. Lin, and J. Ma, 2000: On the seasonal inconsistency of altimeter wind speed algorithms. *Int. J. Remote Sens.*, **21**, 2119–2125.
- Donelan, M. A., M. Skafel, H. Graber, P. Liu, D. Scwhab, and S. Venkatesh, 1992: On the growth rate of wind-generated waves. *Atmos.–Ocean*, **30**, 457–478.
- , F. W. Dobson, S. D. Smith, and R. J. Anderson, 1993: On the dependence of sea surface roughness on wave development. *J. Phys. Oceanogr.*, **23**, 2143–2149.
- Gourrion, J., D. Vandemark, S. Bailey, and B. Chapron, 2002a: Investigation of C-band altimeter cross section dependence on wind speed and sea state. *Can. J. Remote Sens.*, **28**, 484–489.
- , —, —, C. P. Gommenginger, P. G. Challenor, and M. A. Srokosz, 2002b: A two parameter wind speed algorithm for Ku-band altimeters. *J. Atmos. Oceanic Technol.*, **19**, 2030–2048.
- Graber, H. C., N. Ebuchi, and R. Vakkayil, 1996: Evaluation of ERS-1 scatterometer winds with wind and wave ocean buoy obser-

- ventions. Tech. Rep. RSMAS 96-003, Rosenstiel School of Marine and Atmospheric Sciences, University of Florida, Miami, FL, 69 pp.
- Hanson, J. L., and O. M. Phillips, 1999: Wind sea growth and dissipation in the open ocean. *J. Phys. Oceanogr.*, **29**, 1633–1648.
- Keller, W. C., W. C. Wislmann, and W. Alpers, 1989: Tower-based measurements of the ocean C-band radar backscattering cross section. *J. Geophys. Res.*, **94**, 924–930.
- Kitaigorodskii, S. A., 1973: *The Physics of Air–Sea Interaction*. Israel Program for Scientific Translations, 237 pp.
- Queffeulou, P., B. Chapron, and A. Bentamy, 1999: Comparing Ku-band NSCAT scatterometer and ERS-2 altimeter winds. *Trans. Geosci. Remote Sens.*, **37**, 1662–1670.
- Quilfen, Y., B. Chapron, T. Elfouhaily, K. Katsaros, and J. Tournadre, 1998: Observation of tropical cyclones by high resolution scatterometry. *J. Geophys. Res.*, **103**, 7767–7786.
- , —, A. Bentamy, J. Gourrion, T. Elfouhaily, and D. Vandemark, 1999: Global ERS-1/2 and NSCAT observations: Upwind/crosswind and upwind/downwind measurements. *J. Geophys. Res.*, **104**, 11 459–11 469.
- , —, and D. Vandemark, 2001: The ERS scatterometer wind measurement accuracy: Evidence of seasonal and regional biases. *J. Atmos. Oceanic Technol.*, **18**, 1684–1697.
- Vandemark, D., J. B. Edson, and B. Chapron, 1997: Altimeter estimation of sea surface wind stress for light to moderate winds. *J. Atmos. Oceanic Technol.*, **14**, 716–722.
- Weissman, D. E., and H. C. Graber, 1999: Satellite scatterometer studies of ocean surface stress and drag coefficients using a direct model. *J. Geophys. Res.*, **104**, 11 329–11 336.